

Emerging Ultra-Narrow-Band Cyan-Emitting Phosphor in Silicate Materials for White LEDs with Enhanced Color Rendition

Ming Zhao¹, Hongxu Liao¹, Maxim S. Molochev^{2,3,4}, Yayun Zhou⁵, Qinyuan Zhang⁵, Quanlin Liu¹ and Zhiguo Xia^{1,*}

¹The Beijing Municipal Key Laboratory of New Energy Materials and Technologies, School of Materials Sciences and Engineering, University of Science and Technology Beijing, Beijing 100083, China

²Laboratory of Crystal Physics, Kirensky Institute of Physics, Federal Research Center KSC SB RAS, Krasnoyarsk 660036, Russia

³Siberian Federal University, Krasnoyarsk, 660041, Russia

⁴Department of Physics, Far Eastern State Transport University, Khabarovsk, 680021 Russia

⁵State Key Laboratory of Luminescent Materials and Devices and Guangdong Provincial Key Laboratory of Fiber Laser Materials and Applied Techniques, South China University of Technology, Guangzhou 510641, China

Phosphor-converted white LED strategy relies on combining a single blue-emitting InGaN chip with one or more luminescent materials that emit in the remaining part of the visible spectrum, according to the principles of additive colour mixing. The discovery of cyan-emitting (470–500 nm) phosphors is a challenge to realize the full-spectrum white LED lighting. Herein, we reported a ultra-narrow-band cyan-emitting phosphor $\text{Na}_{0.5}\text{K}_{0.5}\text{Li}_3\text{SiO}_4:\text{Eu}^{2+}$ (NKLSO:Eu²⁺), which can be excited by InGaN blue chips and shows cyan emission at 486 nm with a narrow full width at half maximum (FWHM) of only 20 nm, as well as good thermal stability with the integrated emission loss of only 7 % at 150 °C. The unprecedented ultra-narrow band cyan emission results from the highly condensed, rigid framework structure (the degree of condensation $k = 1$) in UCr_4C_4 -type host, and also the high symmetry cations' sites leading to almost ideal cubic coordination. NKLSO:Eu²⁺ phosphor allows for filling the valley between the blue and yellow emission peaks in white LED device, and the color-rendering index can be enhanced from 84.9 to 94.3, suggesting great applications in the full-spectrum white LEDs.

White light-emitting diodes (LEDs) have been widely used in the solid-state lighting or backlight unit for liquid due to high efficiency, tunable color, durability, long lifetime, energy savings, and environmentally friendly.¹⁻³ Currently, the mostly commercial phosphor-converted LED (pc-LEDs) can be achieved by the combination of a blue InGaN chip with yellow-emitting $\text{Y}_3\text{Al}_5\text{O}_{12}:\text{Ce}^{3+}$ (YAG:Ce) phosphor.^{4,5} However, it is acknowledged that such white LEDs have some drawbacks like low color-rendering index (CRI, $R_a < 80$) and high correlated color temperature (CCT > 4000 K) owing to the lack of the red region of spectrum, which is not suitable for high-quality general lighting.⁶ After the discovery of highly efficient red-emitting phosphors, such as $\text{Sr}_2\text{Si}_5\text{N}_8:\text{Eu}^{2+}$, $\text{CaAlSiN}_3:\text{Eu}^{2+}$, $\text{K}_2\text{SiF}_6:\text{Mn}^{4+}$ or $\text{SrLiAl}_3\text{N}_4:\text{Eu}^{2+}$, the R_a values can be enhanced to ~90.⁷⁻¹¹ However, there is still a challenge on the enhanced color rendition because of the cyan gap between blue and yellow in the 470-500 nm region. Hence, it is of fundamental importance to develop a novel phosphor emitting in this spectral region for filling the valley between the blue and yellow emission peaks in white LED device. Accordingly, the development of the narrow-band cyan-emitting

phosphors excited by blue light with small Stokes shift is necessary for improving emission characteristics of state-of-the-art pc-LEDs.^{12,13}

Narrow-band cyan emission plays an important role in enhancing the color rendition based on the compensation of the peak valley between the blue and yellow emission peaks, moreover, the narrow-band emission in this region will also avoid the sacrifice of the maximum achievable luminous efficacy to decrease the spectral overlapping region with blue and yellow emission. Presently, there are few narrow-band cyan-emitting phosphors that can be excited by blue light. The typical example is $\text{BaSi}_2\text{O}_2\text{N}_2:\text{Eu}^{2+}$, which possess an emission band centered at ~ 495 nm with a full width at half maximum (FWHM) of ~32 nm.¹⁴ But it has poor chemical and thermal stability due to the layered crystal structure. Recently, a new narrow-band cyan-emitting oxonitridoberyllate phosphor $\text{Sr}[\text{Be}_6\text{ON}_4]:\text{Eu}^{2+}$ ($\lambda_{\text{em}} = 495$ nm, FWHM = 35 nm) has been reported.¹² However, the harsh synthesis condition and toxicity of this phosphor are serious drawbacks for the application. Therefore, novel stable and non-toxic phosphors with narrow-

band cyan emission are required for the application in enhancing the color rendition.

Nowadays, the development of narrow-emitting phosphors has been continuously pursued for the versatile applications in the field of solid-state lighting or backlight unit for liquid, and the understanding structure-property relations for the creation of narrow-band emission is also a great challenge. Mineral-inspired prototype evolution and new phase construction proposed by our group has demonstrated great potential in the discovery of new phosphors.⁵ For example, the recent report on Be-containing narrow band nitride phosphor, SrLi₂[Be₄O₆] is related with the BaLi₂(Al₂Si₂)N₆] prototype and Sr[BeSi₂N₄] is originated from Sr[Be₃O₆] model, respectively.^{12,13} Accordingly, narrow-band emission nitride phosphors are extensively investigated in UC_rC₄-type model, one of typical examples is red-emitting Sr[LiAl₃N₄]:Eu²⁺ with highly condensed, rigid framework with a degree of condensation $k = 1$, and highly symmetric dopant sites.¹⁰ Therefore, oxide-based UC_rC₄ type compounds with narrow-band emission can be expected. Inspired by these, emerging ultra-narrow-band cyan-emitting phosphor in silicate materials has been firstly demonstrated in this work, and we designed a novel narrow-band cyan-emitting silicate phosphor, [Na_{0.5}K_{0.5}][Li₃Si]O₄, which is originated from UC_rC₄ type compound, NaLi₃SiO₄, in this host family. The relationship between the unprecedented ultra-narrow band cyan emission and three different cations with high symmetry cations' sites leading to almost ideal cubic coordination with equal bond lengths has been analyzed. Eu²⁺ doped [Na_{0.5}K_{0.5}][Li₃Si]O₄ (abbreviated as NKLSO:Eu²⁺) phosphor exhibits an ultra-narrow-band emission with the peak at 486 nm, FWHM = 20 nm and the Stokes shift = 1069 cm⁻¹. Moreover, this phosphor possesses good thermal stability with the integrated emission intensity of 93% at 150 °C. By employing the cyan phosphor NKLSO:Eu²⁺, the commercial yellow phosphor YAG:Ce³⁺ and the commercial red phosphor KSF:Mn⁴⁺ on a blue LED chip, a warm white LED with high R_a of 94.3 was obtained, which demonstrated the phosphor can cover the cyan gap to enhance the CRI in the as-fabricated white LEDs.

Results

Crystal Structure and morphology of NKLSO. The XRD patterns of NKLSO, NKLSO:1%Eu²⁺ are shown in Fig. 1a, and all the diffraction peaks can be indexed to the reported pattern of RbNa₃Li₈(Li(SiO₄))₄ (PDF card No.82-0818)¹⁵, which indicates NKLSO is isostructural to it. Hence, Rietveld refinement was performed to confirm the phase structure. The crystal structure of RbNa₃Li₈(Li(SiO₄))₄¹⁵ was taken as starting model for Rietveld refinement. There are three cations' sites in the host and all of them were occupied by K/Na mixed ions. The ratios were allowed to refine with restriction that sum of occupations occ(Na) + occ(K) are equal to 1 in all sites. After preliminary refinement it was found that first cation is fully occupied by K⁺ ions, second site is intermixed K/Na with the ratio of 0.67/0.33 and third site is fully occupied by Na⁺ ions

(Fig. 1b). These occupations were account in new model and K/Na ratios were fixed in the first and third sites. Thermal parameters of all ions were refined isotropically. Refinement was stable and gives low R -factors (Supplementary Fig. 1 and Supplementary Table 1). It is found that NKLSO crystallizes in a tetragonal crystal system with space group $I4/m$, and its unit cell parameters are $a = b = 10.9447$ (1) Å and $c = 6.26244$ (8) Å. Coordinates of atoms and main bond lengths are shown in Supplementary Table 2 and Supplementary Table 3 respectively. Chemical formula from refinement can be written as Na_{0.58(4)}K_{0.42(4)}Li₃SiO₄ which is close to suggested formula within 2σ. The crystallographic information file (CIF) of NKLSO is also presented in the Supporting Information. As for crystal structure (Fig. 1b and Supplementary Fig. 2), LiO₄ and SiO₄ tetrahedra connected to each other by corner- and edge-sharing to form a highly condensed three-dimensional framework with the degree of condensation $\kappa = 1$ (i.e., atomic ratio (Li, Si): O = 1), and three different cations, K1, K2/Na2 and Na3 are filled in *vierer* ring channels along [001]. All of these ions are coordinated by eight O²⁻ ions forming cubic polyhedron with high symmetry character (Fig. 1b). Such as a high symmetry 4/ m of K1 and K2/Na2 sites lead to almost ideal cubic coordination with equal $d_{(Na,K-O)}$ bond lengths and with difference between some $d_{(O-O)}$ only (Fig. 1b), which extremely contribute to the as-observed narrow emission bands, as also discussed below. The Na3 site has relatively low symmetry -4 and bond lengths $d_{(Na3-O)}$ divide into two groups leading to distorting cubic coordination.

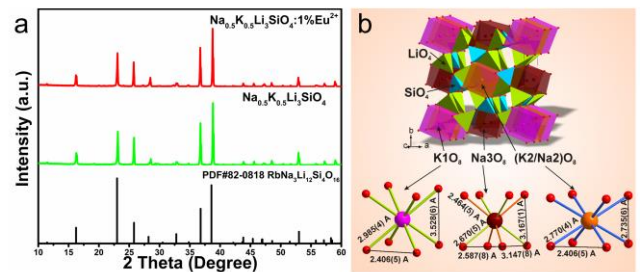


Figure 1 | Crystal structure of NKLSO:Eu²⁺ phosphor. (a) XRD patterns of NKLSO, NKLSO:1%Eu²⁺ and standard pattern of PDF card No.82-0818 as reference. (b) Crystal structure of Na_{0.5}K_{0.5}Li₃SiO₄ and the coordination spheres of K1, Na3, and K2/Na2.

The local structure, chemical composition and morphology of NKLSO:Eu²⁺ phosphor have been further investigated to check this newly discovered ultra-narrow band cyan-emitting phosphor. Firstly, the ⁷Li NMR spectrum was measured. As displayed in Fig. 2a, the ⁷Li NMR spectrum shows two signals at 2.721 and 4.402 ppm, which is consistent with two different Li crystallographic sites in this host. Scanning electron microscope (SEM) images of NKLSO powder sample are depicted in Fig. 2b and 2c, which indicates the average particle size of the sample is about 5~10 μm, and well developed crystalline particle and smooth surface will help to the luminescence property and the LED package technique. The elemental mapping images (Fig. 2d) show uniform distribution of Na, K, Si,

and O elements in the particle, and the average atomic ratios Na(0.5):K(0.44):Si(1.1) determined by energy dispersive X-ray spectroscopy (EDS) are in accordance with the formula $\text{Na}_{0.58(4)}\text{K}_{0.42(4)}\text{Li}_3\text{SiO}_4$ obtained from the Rietveld refinement result from XRD pattern.

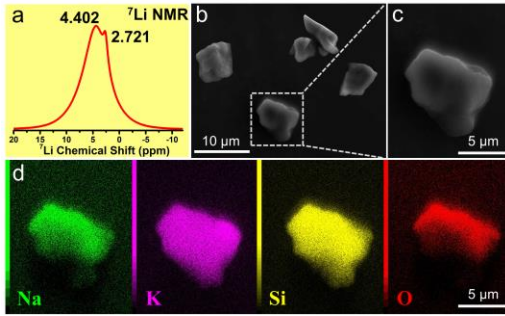


Figure 2 | The composition and morphology of NKLSO:Eu²⁺ phosphor. (a) The ⁷Li solid-state NMR spectrum of NKLSO. (b) SEM image of NKLSO microcrystal particles and (c) an enlarged particle. (d) EDS elemental mapping images of the selected NKLSO particle.

Photoluminescence Properties. The diffuse reflectance, photoluminescence excitation (PLE) and emission (PL) spectra of NKLSO:Eu²⁺ phosphor are shown in Fig. 3. The PLE spectra monitoring by two different wavelength, 486 and 510 nm, show a broad band from 300 to 500 nm, indicating it can be excited by UV to blue light and suitable for excitation of the commercial blue chip. The diffuse reflectance spectrum shows a broad absorption band over the 330–470 nm, which matched well with the excitation spectrum. The PL spectrum of the NKLSO:Eu²⁺ phosphor consists of a dominate asymmetric narrow-band peak at 486 nm with FWHM of only 20 nm and a minor shoulder peak at 530 nm under 400 nm excitation, indicating it may exist different luminescence centers which will be discussed later. The inset image shows the sample has a cyan light under 365 nm lamp irradiation. The highly condensed and rigid network result in the narrow-band emission and the small Stokes shift which is determined as the energy difference between the maximum of the (lowest) excitation band and that of the emission band.¹⁶ Hence, the extremely small Stokes shift (1069 cm⁻¹) of NKLSO:Eu²⁺ also accounts for the confinement in the local structure relaxation of Eu²⁺ in its excited state.

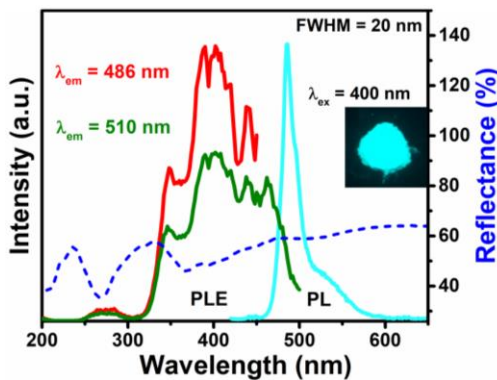


Figure 3 | Photoluminescence properties of NKLSO:Eu²⁺ phosphor. Diffuse reflectance, photoluminescence excitation and emission spectra of NKLSO:Eu²⁺. The inset shows digital photograph of cyan NKLSO:Eu²⁺ phosphor under 365 nm UV lamp.

To further verify the correlation between the existed luminescent centers and the crystallographic sites in the crystal structure, the PL spectrum at 80 K of NKLSO:Eu²⁺ were measured. It is commonly known that fine emission spectrum can be observed at the low temperature owing to the reduce of thermal broadening. As shown in Fig. 4a, three emission bands located at 486 nm, 495 nm, and 529 nm are clearly observed, which can be attributed to the existence of three luminescence centers, originated from three cation sites occupied by Eu²⁺, as elucidated in the crystal structure analysis. Furthermore, the PL spectrum at 80 K can be divided into three Gaussian peaks (Fig. 4a). Two narrow peaks with FWHM~4.5/14.3 nm can be associated with K1 and K2/Na2 sites occupied by Eu²⁺ because they located in the highly cubic symmetry sites, and the slightly wide emission band with FWHM~52.4 nm can be associated with Na3 sites occupied by Eu²⁺ owing to the distorting cubic sites. In order to further understand the origin of the three emission bands, the well-known experiential equation given by Van Uitert can be used, which provides a good fit to the emission peak for Eu²⁺ and Ce³⁺.¹⁷

$$E = Q \left[1 - \left(\frac{V}{4} \right)^{\frac{1}{V}} 10^{-\frac{n \times EA \times r}{80}} \right] \quad (1)$$

where E represents the position of the d-band edge in energy for rare earth ions (cm⁻¹), Q is the position in energy for the lower d-band edge for the free ions, value of Q is 34000 cm⁻¹ for Eu²⁺ and 50000 cm⁻¹, V is the valence of the active ion, here $V = 2$, n is the number of anions in the immediate shell about this ion, EA is the electron affinity of the atoms that form anions, and r is the radius of the host cation replaced by the active cation. Here, $n = 8$ for K1, K2/Na2 and Na3 sites, EA should act as the same values for K1, K2/Na2 and Na3 in this host, and $r(\text{K1}) > r(\text{K2/Na2}) > r(\text{Na3})$. Form the equation, we can know that the bigger the r is, the bigger the E , and the smaller the emission wavelength. Hence, the first peak (486 nm) in PL spectrum can be assigned to K1 sites, the second peak (495 nm) can be assigned to K2/Na2 sites, and the third broad peak (529 nm) can be assigned to Na3 sites, which is consistent with the previous analysis results depending on different symmetry. Moreover, decay behaviors of Eu²⁺ at various sites are generally different depending on variable chemical environment. To further confirm the presence of three Eu²⁺ emissions in NKLSO:Eu²⁺, the decay curves at 80 K monitored at 486, 495, and 529 nm under 400 nm excitation are measured (Fig. 4b). The lifetimes are calculated to be 0.843, 0.852, and 0.965 μs for peaks at 486, 495 and 529 nm, respectively. The different decay time values demonstrated that the emissions arise from Eu²⁺ in different lattice sites and the close lifetimes (0.843 and 0.852 μs) is ascribed to the quite

similar $4/m$ sites (K1, K2/Na) in the lattice, while the value of $0.965 \mu\text{s}$ should be ascribed to Eu^{2+} at the different Na3 site with relatively low symmetry -4.

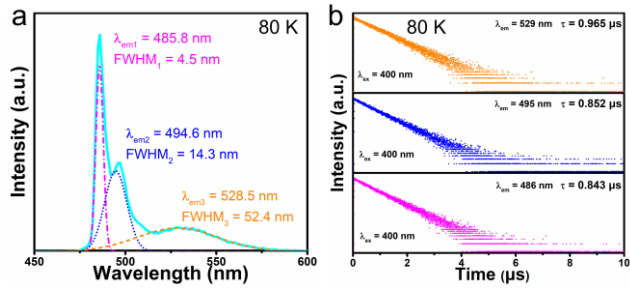


Figure 4 | Photoluminescence properties of NKLSO:Eu²⁺ phosphor at 80 K. (a) Photoluminescence emission spectra of NKLSO:Eu²⁺ at 80 K. (b) The decay curves at 80 K of NKLSO:Eu²⁺ under excitation at 400 nm, monitored at different wavelengths.

Thermal Quenching Properties. The thermal stability is a crucial parameter for LED phosphors in the practical application, since the LED chip normally reaches temperature up to $\sim 150^\circ\text{C}$ at high power. The behaviour of thermal quenching can be explained using the configurational coordinate diagram, in which the excited luminescent centre is thermally activated through phonon interaction and then released through the crossing point between excited and ground states.¹⁸ Hence, thermal quenching is related to the difference between the equilibrium distance of the ground- and excited-state (ΔR) in the configurational coordinate diagram, which determines the location of the crossing point.¹⁹ It is clear that the smaller the value of ΔR is, the smaller the Stokes shift.¹⁶ Generally, the phosphor with the smaller Stokes shift has stronger structural rigidity,²⁰ which could significantly reduce the emission loss with increasing temperature. The temperature-dependent emission spectra of NKLSO:Eu²⁺ phosphor in the temperature range room temperature (RT) to 250°C are shown in Fig. 5a. At 150°C , NKLSO:Eu²⁺ exhibits the integrated emission loss of only 7% and the emission intensity of the peak (486 nm) is lost 25% of the initial intensity, indicating a good thermal stability of NKLSO:Eu²⁺ (Fig. 5b). The difference between the integrated intensity and the intensity of 486 nm is attributed to the broadening of the emission band with the increasing temperature.

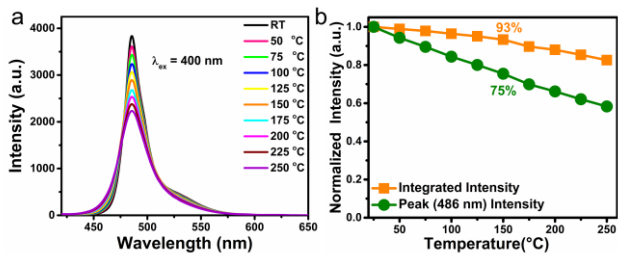


Figure 5 | Thermal quenching behavior of NKLSO:Eu²⁺ phosphor. (a) Temperature-dependent emission spectra of NKLSO:Eu²⁺ phosphor under 400 nm excitation in the temperature range RT– 250°C with a temperature interval of 25°C . (b)

Temperature-dependent normalized integrated PL intensities and normalized the peak (486 nm) intensities of NKLSO:Eu²⁺.

Performance of as-fabricated white LEDs for enhancing color rendition. To further evaluate the potential application of NKLSO:Eu²⁺ in white LEDs lighting for improving color rendering index, we fabricated white LED lamps by using the cyan phosphor NKLSO:Eu²⁺, the commercial yellow phosphor YAG:Ce³⁺ and the commercial red phosphor KSF:Mn⁴⁺ on a blue LED InGaN chip ($\lambda = 455 \text{ nm}$) under various drive currents, compared with the white LED without the cyan phosphor NKLSO:Eu²⁺. Fig. 6a and 6b comparatively show the EL spectra of the as-fabricated LED1 (without the sample) and LED2 (with the sample) devices under a current of 20 mA, and the insets show the photographs of the fabricated and lightened white LEDs. The LED1 presents warm white light with the correlated color temperature (CCT) of 3818K, the color render index (R_a) of 84.9 and chromaticity coordinates of (0.3912, 0.3896). However, the LED 1 shows a cyan gap causing the limited enhancement of the color rendering index (R_a), which is difficult to beyond 90. As the cyan phosphor NKLSO:Eu²⁺ was added into the device, the LED2 shows the similar CCT of 3797 K and chromaticity coordinates of (0.3905, 0.3845), but the color rendering index (R_a) can be enhanced to 94.3, indicating the great application potential of the device in full-spectrum lighting for enhancing color rendition. The EL spectra and the variation in chromaticity coordinates of the white LED devices under various drive current are shown in Supplementary Fig. 3, and Supplementary Table 4 and Supplementary Table 5, and some photoelectric parameters are provided also showing that the chromaticity coordinates of LED1 shift more than LED2 indicating the LED2 have better color stability when the drive current increases from 20 to 300 mA.

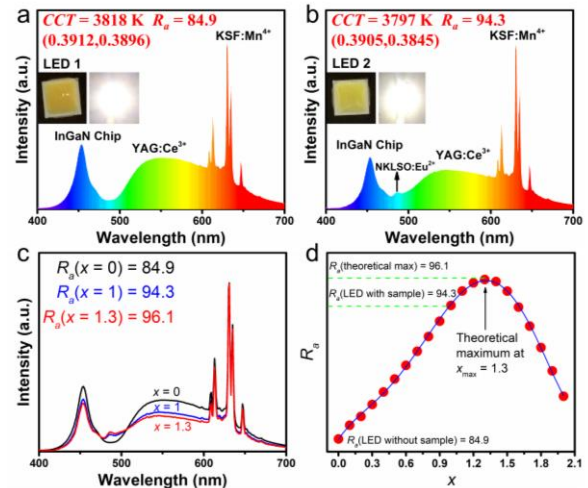


Figure 6 | Performance of as-fabricated white LED devices. EL spectra of the white LED devices fabricated with the commercial yellow phosphor YAG:Ce³⁺, the commercial red phosphor KSF:Mn⁴⁺ and without (a) or with (b) the cyan phosphor NKLSO:Eu²⁺ on a blue LED InGaN chip ($\lambda = 455 \text{ nm}$) under a current of 20 mA. The inset show the photographs of fabricated

white LEDs. (c) Experimental spectra of white LED without the sample ($x = 0$), WLED with the sample ($x = 1$) and theoretical spectrum $x = 1.3$. (d) The R_a index plot per x for different theoretical spectra, $\text{THEOR}(\lambda) = \text{LED1}(\lambda) + x \times \text{DIFF}(\lambda)$ with maximum at $x = 1.3$ and theoretical maximum R_a (theoretical max) = 96.1.

Discussion

Based on the comparison of the EL spectra of LED1 and LED2 (Fig. 6c), it reveals three main features: 1) additional peak appears at about 490 nm in spectrum of the LED2, and it really compensates cyan gap between 470-500 nm; 2) this cyan-emitting spectrum shows the decrease of intensity of two peaks at 455 nm and 550 nm, indicating the noticeable increasing absorption of blue part in the range of 380-600 nm; 3) narrow high-intensity peaks in the range of 600-650 nm stay almost invariable, causing the relative intensity of red part increasing compared with the blue part. The character of spectra change is complex and in order to predict theoretical maximum of R_a , first of all, it was decided to calculate the difference between the spectra: $\text{DIFF}(\lambda) = \text{LED2}(\lambda) - \text{LED1}(\lambda)$, where $\text{LED2}(\lambda)$ is the experimental spectrum of the LED2, $\text{LED1}(\lambda)$ is the experimental spectrum of the LED1. The different theoretical spectrum $\text{THEOR}(\lambda)$ therefore can be presented as sum of spectrum $\text{LED1}(\lambda)$ without sample and additions of $\text{DIFF}(\lambda)$ with scaling coefficient x : $\text{THEOR}(\lambda) = \text{LED1}(\lambda) + x \times \text{DIFF}(\lambda)$. It should be noted that $x = 0$ means pure $\text{LED1}(\lambda)$ spectrum and $x = 1$ is pure $\text{LED2}(\lambda)$ spectrum. Several theoretical spectra were obtained by varying x in the range of $x = 0 \dots 2$ with the step 0.1. The R_a index of each spectrum was calculated and the dependence of R_a on x was plotted (Fig. 6d). It was found the maximum in $R_a(x)$ function is $x = 1.3$ with $R_a(\text{max}) = 96.1$. Therefore, the R_a of LED with cyan phosphor NKLSO:Eu^{2+} can be raised to 96.1 and the fabricated LED2 with $R_a = 94.3$ is close to this maximum (Fig. 6d). The spectra with such theoretical maximum was calculated using the equation of $\text{THEOR}(\lambda)$ and $x = 1.3$ value, and it also showed similarity with the spectrum of LED2 (Fig. 6c), which indicates the theoretical prediction is reasonable.

In summary, we have successfully designed and synthesized a novel ultra-narrow-band cyan-emitting NKLSO:Eu^{2+} phosphor with $\lambda_{\text{em}} = 486$ nm, FWHM of only 20 nm and Stokes shift of 1069 cm^{-1} . The extremely small Stokes shift and unprecedented ultra-narrow-band cyan emission is attributed to the highly condensed, rigid framework and highly cubic symmetry sites for the activator (Eu^{2+}). The cyan-emitting phosphor also shows good thermal stability with the integrated emission intensity of 93% at $150 \text{ }^\circ\text{C}$, demonstrating NKLSO:Eu^{2+} is a promising for pc-LEDs for enhancing the color rendering index as full-spectrum lighting application. By combining this newly-discovered cyan phosphor NKLSO:Eu^{2+} , the commercial yellow phosphor YAG:Ce^{3+} and the commercial red phosphor KSF:Mn^{4+} with a blue InGaN LED chip, we fabricated a warm white LED with R_a of 94.3. Compared with the white LED without the NKLSO:Eu^{2+} , the R_a has been im-

proved significantly, indicating the phosphor can compensate for the cyan gap and demonstrate great potential to the high-CRI white LEDs devices.

Methods

Materials and Preparation. The powder samples of NKLSO:Eu^{2+} were synthesized by the traditional solid-state reaction. Stoichiometric amounts of Na_2CO_3 (A.R., Aladdin), K_2CO_3 (A.R., Aladdin), Li_2CO_3 (A.R., Aladdin), SiO_2 (A.R., Aladdin), and Eu_2O_3 (99.99%, Aladdin) were homogeneously mixed and ground with ethanol for half an hour. The mixtures were first sintered at 550°C for 5h in air and then sintered 3 times at 750°C for 4 h under a reducing atmosphere of H_2 (10%) and N_2 (90%) in a tube furnace. After cooling to room temperature, the obtained samples were reground into fine powders for further characterization.

Characterization. The powder X-ray diffraction (XRD) data of NKLSO for Rietveld analysis was collected at room temperature by a Bruker D8 ADVANCE powder diffractometer with monochromatized $\text{Cu K}\alpha$ radiation ($\lambda = 1.5406 \text{ \AA}$) at 40 kV and 40 mA. Rietveld refinement was performed by using TOPAS 4.2. The morphology of the powder sample was observed by scanning electron microscope (SEM, JEOL JSM-6510). The elemental composition and elemental mapping were obtained using energy dispersive X-ray spectroscopy (EDS) that was attached to the SEM. The diffuse reflectance spectra at room temperature were measured on a Hitachi UH4150 ultraviolet-visible-near infrared spectrophotometer and using white BaSO_4 for calibration. The photoluminescence excitation (PLE) and photoluminescence emission (PL) spectra at room temperature were recorded by an Edinburgh FLS920 fluorescence spectrophotometer with the Xe900 lamp as the excitation source. The luminescence decay curves were obtained by the FLS920 using an nF900 flash lamp as the excitation source. For low-temperature (80 K) measurements, sample was cooled in a liquid nitrogen cryostat on Oxford Instruments that was attached to the FLS920. The temperature-dependent spectra were measured by a Hitachi F-4600 fluorescence spectrophotometer with a heating apparatus as heating source and a 150 W Xe lamp as the excitation source.

WLEDs fabrication. White light-emitting diodes (LEDs) were fabricated with the cyan phosphor NKLSO:Eu^{2+} , the commercial yellow phosphor YAG:Ce^{3+} , the commercial red phosphor KSF:Mn^{4+} and a blue LED InGaN chip ($\lambda = 455 \text{ nm}$). The phosphors were thoroughly mixed with epoxy resin, and the obtained phosphor-epoxy resin mixture was coated on the LED chips. The photoelectric properties, including the electroluminescence (EL) spectra, color temperature (CCT), color rendering index (CRI, R_a), luminous efficacy and CIE color coordinates of the LEDs, were measured by using an integrating sphere spectroradiometer system (ATA100, Ever fine).

REFERENCES

1. Pust, P., Schmidt, P. J., Schnick, W. A revolution in lighting. *Nat. Mater.* **14**, 454 (2015).
2. Pimpitkar, S., Speck, J. S., DenBaars, S. P., Nakamura, S. Prospects for LED lighting. *Nat. Photonics* **3**, 180 (2009).
3. Schubert, E. F., Kim, J. K. Solid-state light sources getting smart. *Science* **308**, 1274-1278 (2005).
4. Xia, Z. G., Meijerink, A. Ce³⁺-Doped garnet phosphors: composition modification, luminescence properties and applications. *Chem. Soc. Rev.* **46**, 275-299 (2017).
5. Xia, Z. G., Liu, Q. L. Progress in discovery and structural design of color conversion phosphors for LEDs. *Prog. Mater. Sci.* **84**, 59-117 (2016).
6. Meyer, J., Tappe, F. Photoluminescent Materials for Solid-State Lighting: State of the Art and Future Challenges. *Adv. Opt. Mater.* **3**, 424-430 (2015).
7. Huang, L., *et al.* HF-Free Hydrothermal Route for Synthesis of Highly Efficient Narrow-Band Red Emitting Phosphor K₂Si_{1-x}F_{6-x}Mn⁴⁺ for Warm White Light-Emitting Diodes. *Chem. Mater.* **28**, 1495-1502 (2016).
8. Xie, R.-J., Hirosaki, N., Suehiro, T., Xu, F.-F., Mitomo, M. A Simple, Efficient Synthetic Route to Sr₂Si₅N₈:Eu²⁺-Based Red Phosphors for White Light-Emitting Diodes. *Chem. Mater.* **18**, 5578-5583 (2006).
9. Piao, X., Machida, K.-i., Horikawa, T., Hanzawa, H., Shimomura, Y., Kijima, N. Preparation of CaAlSiN₃:Eu²⁺ Phosphors by the Self-Propagating High-Temperature Synthesis and Their Luminescent Properties. *Chem. Mater.* **19**, 4592-4599 (2007).
10. Pust, P., *et al.* Narrow-band red-emitting Sr[LiAl₃N₄]:Eu²⁺ as a next-generation LED-phosphor material. *Nat. Mater.* **13**, 891-896 (2014).
11. Wang, L., *et al.* Ca_{1-x}Li_xAl_{1-x}Si_{1+x}N₃:Eu²⁺ solid solutions as broadband, color-tunable and thermally robust red phosphors for superior color rendition white light-emitting diodes. *Light: Sci. Appl.* **5**, e16155 (2016).
12. Strobel, P., de Boer, T., Weiler, V., Schmidt, P. J., Moewes, A., Schnick, W. Luminescence of an Oxonitridoberyllate: A Study of Narrow-Band Cyan-Emitting Sr[Be₆ON₄]:Eu²⁺. *Chem. Mater.* **30**, 3122-3130 (2018).
13. Strobel, P., Maak, C., Weiler, V., Schmidt, P. J., Schnick, W. Ultra-Narrow Band Blue Emitting Oxoberyllates AELi₂[Be₄O₆]:Eu²⁺ (AE = Sr,Ba) Paving the Way to Efficient RGB pc-LEDs. *Angew Chem Int Ed Engl*, (2018).
14. Li, Y. Q., Delsing, A. C. A., de With, G., Hintzen, H. T. Luminescence Properties of Eu²⁺-Activated Alkaline-Earth Silicon-Oxynitride MSi₂O_{2-δ}N_{2+2/3δ} (M = Ca, Sr, Ba): A Promising Class of Novel LED Conversion Phosphors. *Chem. Mater.* **17**, 3242-3248 (2005).
15. Hoffmann, J., Brandes, R., Hoppe, R. Neue Silicate mit „Stuffed Pyrgoms“□: CsKNaLi₉{Li[SiO₄]}₄, CsKNa₂Li₈{Li[SiO₄]}₄, RbNa₃Li₈{Li[SiO₄]}₄ [1] und RbNaLi₄{Li[SiO₄]}₂ [2]. *Z. Anorg. Allg. Chem.* **620**, 1495-1508 (1994).
16. Blasse, G., Grabmaier, B. C. In: *Luminescent Materials* (ed[^](eds). Springer Berlin Heidelberg (1994).
17. Van Uitert, L. G. An empirical relation fitting the position in energy of the lower d-band edge for Eu²⁺ or Ce³⁺ in various compounds. *J. Lumin.* **29**, 1-9 (1984).
18. Kim, Y. H., *et al.* A zero-thermal-quenching phosphor. *Nat. Mater.* **16**, 543-550 (2017).
19. Blasse, G. Thermal quenching of characteristic fluorescence. *J. Chem. Phys.* **51**, 3529-3530 (1969).
20. Denault, K. A., *et al.* Average and local structure, Debye temperature, and structural rigidity in some oxide compounds related to phosphor hosts. *ACS Appl. Mater. Interfaces* **7**, 7264-7272 (2015).

Corresponding Author

* E-mail: xiazg@ustb.edu.cn

Acknowledgement

The present work was supported by the National Natural Science Foundations of China (Grant Nos. 51722202, 91622125 and 51572023), Natural Science Foundations of Beijing (2172036) and RFBR (Grant No. 17-52-53031).

Author contributions

Z. G. X initiated and guided the research. M. Z and Z. G. X discussed and wrote the manuscript, and Q. L. L. revised and commented on it. M. Z and H. X. L. performed the experiments. M. S. M performed Rietveld refinement of power X-ray diffraction results. Y. Y. Z and Q. Y. Z. fabricated the WLEDs and analyzed the EL spectra.

Additional information

Supplementary Information accompanies this paper at <http://www.nature.com/naturecommunications>

Competing financial interests

The authors declare no competing financial interests.